Deep-level nitrogen centers in laser-annealed ion-implanted silicon

K. L. Brower
Sandia National Laboratories, Albuquerque, New Mexico 87185
(Received 21 July 1982)

An electron-paramagnetic-resonance (EPR) study dealing with the means for introducing substitutional N into silicon and the structure of N centers is presented in this paper. Nitrogen can be introduced into crystalline silicon by N^+ implantation and subsequent pulsed-ruby-laser annealing. The primary criteria for introducing substitutional N in silicon are that enough energy be supplied during pulsed-ruby-laser annealing to melt the implanted region and that crystalline silicon regrowth occurs. The fraction of the implanted N observed by EPR to be incorporated into substitutional sites (labeled SL5) was measured as a function of N^+ implant energy, N^+ fluence, and laser annealing energy, and was found to be $\lesssim 10\%$. Residual implantation lattice damage is tentatively believed to enhance the formation of other N-defect centers (SL6, SL7) upon thermal annealing between 400 and 450 °C. Unlike the other group-V impurities (P, As, Sb, Bi), substitutional N is observed to be a deep-level impurity with axial symmetry about a $\langle 111 \rangle$ (C_{3v} symmetry) direction. The characteristic reorientation time of the SL5 center is reasonably well described by the Arrhenius expression $\tau = \tau_0 \exp(E/k_B T)$ over the measured temperature region $35 \lesssim T \lesssim 200$ K with $E = 0.107 \pm 0.02$ eV and $\tau_0 \sim 3 \times 10^{-12}$ sec. The reorientation of the SL5 center is enhanced under illumination at low temperatures by (near-) band-gap incandescent light. Contrary to our prior assertion, the position of the N-donor level in the band gap remains unknown. The axial symmetry of the substitutional N center is attributed to a distortion in the positions of the substitutional N and neighboring silicon atoms. Possible explanations for this distortion are reviewed.

I. INTRODUCTION

Recently, we reported[1] the discovery of an electron-paramagnetic-resonance (EPR) spectrum due to substitutional nitrogen that had been introduced into silicon by ion implantation and laser annealing. Unlike the other group-V impurities (P,As,Sb,Bi) in silicon that are shallow donors with T_d symmetry, we observed that nitrogen in silicon is a deep-level impurity with C_{3v} symmetry.[1] In this sense N in silicon is similar to N in diamond.[2] Previous studies have indicated that N in silicon exhibits a complexity of chemical and electrical behavior that is not well understood.[3–7]

Two major aspects of our work on nitrogen in silicon are emphasized in this paper. The first aspect of this paper deals with an extensive exploration of techniques and conditions under which paramagnetic nitrogen centers can be introduced into silicon (Sec. III). The second aspect of our work deals with the identification of these N centers. Here we have applied the techniques of EPR (Sec. IV). Our current understanding of N centers in silicon is summarized in Sec. V. We begin with a brief description of our experimental techniques (Sec. II).

II. EXPERIMENTAL TECHNIQUES

Single-crystal silicon samples used in this experiment were extracted from vacuum—float-zone—grown ingots which were intrinsic with resistivities between 2500 and 4500 Ω cm (p-type). Ion implantation of specific isotopes of N as well as C, O, Al, Si, P, S, or Ge was accomplished with an Accelerators, Inc., 300-keV ion accelerator with magnetic ion-mass separation. The ion current density incident on our samples was $\lesssim 1\ \mu A/cm^2$.

All laser anneals were made with a Q-switched ruby laser ($\lambda = 695.4$ nm) with a Gaussian-type pulse having a full width of 20 ns at half maximum. Spatial variations in beam intensity were homogenized by transmitting the beam through a fused silica rod having a 90° bend with an input diameter of 14.3 mm and an output diameter of 8.6 mm.[8] The samples, whose surfaces had typically a $\frac{1}{4}$-μm polish, were laser annealed with energy densities $\lesssim 3$ J/cm^2. For energy densities $\gtrsim 3$ J/cm^2 the silicon surface was observed to become pitted due to blow-off.

The EPR measurements were made with a K-band superheterodyne spectrometer.[9] In the laser-

annealed, N-implanted samples, the N spectra could be observed unsaturated in the absorption mode for microwave powers of $\lesssim -60$ dBm incident upon the TE_{011} cylindrical cavity at 10 K. The intensity of the N spectrum labeled SL5 was observed to be proportional to $1/T$ for temperatures up to at least 130 K. The absolute number of paramagnetic N centers was determined relative to the known number of free conduction electrons in a spin standard of crushed degenerate silicon embedded in polyethylene which was prepared and supplied by E. A. Gere. The uncertainty in the relative intensity of the N spectra was typically $\lesssim \pm 10\%$; however, the absolute spin density of our N centers is estimated to be uncertain by a factor $\lesssim 2$ ($+100\%$, -50%).

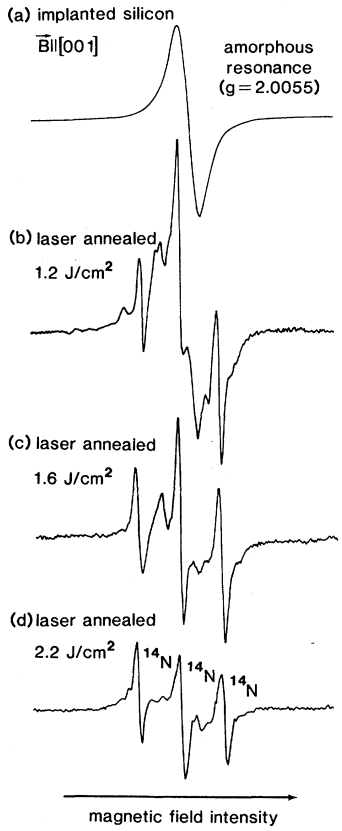

FIG. 1. (a) EPR spectrum observed in silicon implanted with 2×10^{15} 200-keV $^{28}Si^+/cm^2$. This implant produces an amorphous layer that gives rise to the amorphous resonance. The decrease in the paramagnetic lattice damage and the appearance of the ^{14}N spectrum with increasing laser-anneal energy is shown in traces (b)–(d). The N was introduced unintentionally into silicon during implantation as a result of contamination of the $^{28}Si^+$ beam with $^{14}N_2{}^+$. These spectra were observed for $\vec{B}||[001]$.

III. METHODS FOR INCORPORATING N INTO SILICON

A. Laser annealing of amorphous silicon containing nitrogen

In our earliest experiments[10] crystalline silicon (*c*-Si) was made amorphous by implantation with 200-keV $^{28}Si^+$ giving rise to the amorphous resonance shown in Fig. 1(a). Although Rutherford-backscattering measurements indicated that crystallinity of the implanted layer was restored by pulsed-ruby-laser annealing for energies $\gtrsim 1.8$ J/cm^2 (Ref. 10), EPR measurements, which also confirmed the single-crystal character of the implanted region, revealed a hyperfine (hf) spectrum due to ^{14}N as shown in Figs. 1(b)–1(d). ^{14}N has a nuclear spin of 1, giving $2I+1$ hf lines, and is 99.6% naturally abundant. This spectrum and corresponding center are labeled SL5.

Several possible sources of the N were considered: (1) $^{14}N_2{}^+$ contamination of the $^{28}Si^+$ beam, (2) gettering of N_2 during laser annealing in air, (3) passivation of the amorphous silicon (*a*-Si) surface by N_2 after implantation, and (4) adsorbed N_2 recoiled into the silicon during ion implantation. Several experiments were done to identify the source of nitrogen.

Passivation of the *a*-Si surface by N_2 after implantation was not the source of our ^{14}N spectrum. In particular, the target chamber was backfilled to 1 atm with $^{15}N_2$ immediately after ion implantation with $^{28}Si^+$. After laser annealing only the usual ^{14}N

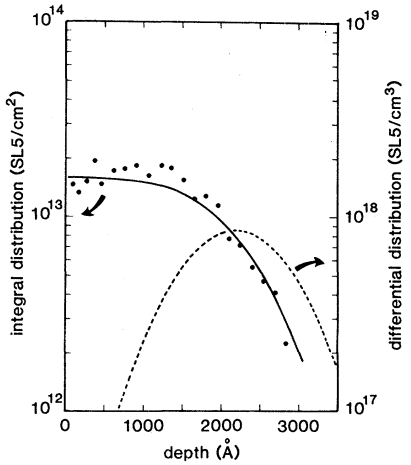

FIG. 2. Depth distribution resulting from implanting 160-keV $^{28}Si^+$ and $^{14}N_2{}^+$ into silicon followed by a pulsed-ruby-laser anneal of 2 J/cm^2 as measured by EPR (dots) and calculated [solid and dashed lines (Refs. 11 and 12)].

hf spectrum was observed: no ^{15}N was detected by EPR.

Gettering of N_2 during laser annealing in air was not the source of nitrogen that we observed with EPR. A sample made amorphous by implantation with ^{28}Si was laser annealed in $^{15}N_2$ gas at 1 atm. Again, only the ^{14}N hf spectrum was observed; no ^{15}N could be detected by EPR.

The integral depth distribution of the ^{14}N as measured by EPR in a *c*-Si sample made amorphous by $^{28}Si^+$ implantation and subsequently laser annealed is shown in Fig. 2. After each succeeding layer of silicon had been removed by anodic oxidation and etching in hydrofluoric acid, the number of SL5 centers remaining in the silicon was measured by EPR. The thickness of each layer of silicon removed versus voltage change for this particular process had been calibrated previously from backscattering studies.[13] Our measurements show, as illustrated in Fig. 2, that the integral distribution of the SL5 center matches that for $^{14}N_2{}^+$ implanted with the same energy as the $^{28}Si^+$. Furthermore, the corresponding differential distribution of N does not correspond to that expected from adsorbed N recoiled from the surface into the silicon during ion implantation. The N distribution arising from this mechanism would have a monotonically decreasing profile contained mostly within 1000 Å from the surface.[14]

If the silicon is made amorphous by implantation of either $^{30}Si^+$ or Ge^+ while keeping all other conditions and procedures the same, no N spectra are observed after laser annealing. In addition to identifying the source of N in our samples, these experiments indicate that the only manner in which detectable amounts of nitrogen are incorporated into SL5 centers during ion implantation and subsequent laser annealing is by *direct* nitrogen implantation.

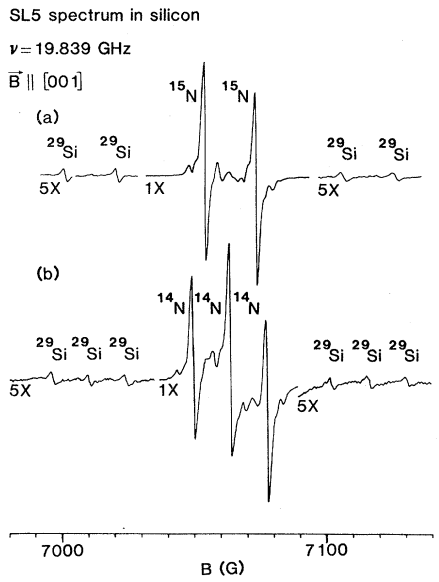

FIG. 3. Si-SL5 EPR spectrum observed in silicon implanted with (a) ^{15}N ($I=\frac{1}{2}$) and (b) ^{14}N ($I=1$) after pulsed-ruby-laser annealing.

B. Laser annealing of crystalline silicon containing nitrogen

A natural extension to the preceding method was to implant only N^+ into crystalline silicon without making it amorphous, followed by laser annealing. In particular, a silicon sample was implanted with 5×10^{15} 205-keV $^{15}N^+/cm^2$ and subsequently pulsed-ruby-laser annealed with 2.6 J/cm^2. The EPR spectrum observed from this sample is shown in Fig. 3(a). Since ^{15}N, which is only 0.365% naturally abundant, has a nuclear spin of $\frac{1}{2}$, the ^{15}N hf spectrum consists of two lines. Furthermore, the ratio in the ^{14}N to ^{15}N hf interactions, $A_{iso}(^{14}N)/A_{iso}(^{15}N)$, as measured experimentally is 0.716 and matches the theoretical ratio of 0.713 to within 0.5%. These results indicate unambiguously that the impurity in the SL5 center is nitrogen.

Our measurements indicate that only a small fraction of the nitrogen implanted into crystalline silicon appears in the form of SL5 centers after laser annealing. The intensity of the SL5 spectrum in Fig. 3(a) corresponds to 1.26×10^{14} SL5 centers per cm^2. In this case only $\simeq$2.5% of the implanted N is contained in *paramagnetic* substitutional sites. This result is consistent with the results obtained from nuclear reaction studies by Mitchell *et al.*,[6]

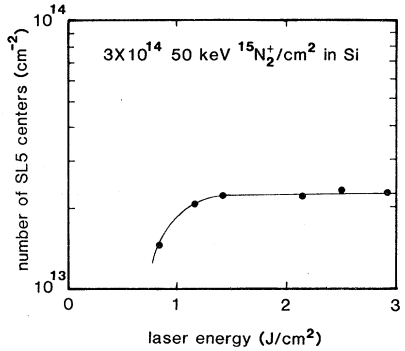

FIG. 4. Number of SL5 centers per cm^2 plotted vs pulsed-ruby-laser energies for fixed $^{15}N_2{}^+$ energy and fluence.

which indicated that less than 5%, if any, of the implanted N was substitutional after thermal annealing.

We explored the effectiveness of introducing N into SL5 centers as a function of laser-anneal energy, nitrogen fluence, and implant energy. For silicon implanted with 3×10^{14} 50-keV $^{15}N_2^+/cm^2$, the number of SL5 centers per cm^2 versus laser energy is plotted in Fig. 4. The energy threshold for melting silicon at the surface with a pulsed ruby laser is $\simeq$0.8 J/cm^2 (Refs. 15 and 16). At 1.15 J/cm^2 calculations indicate that the melt front reaches a depth of $\simeq$1250 Å and passes through $\simeq$97% of the implanted N. These results suggest that a small fraction of the implanted N is incorporated into SL5 centers upon crystalline regrowth from the melt. According to this explanation, the number of SL5 centers for laser-anneal energies between 1.4 and 3 J/cm^2 does not increase because the melt front, which reaches a depth of 1 μm at 3 J/cm^2, extends beyond the region containing essentially all of the implanted N. Since the implanted N is believed to be quenched into substitutional sites upon crystalline regrowth from the melt, the prior state of the implanted region, whether it is amorphous or crystalline, is irrelevant to this process.

We also observe that the SL5 spectrum is more easily saturated in samples annealed with higher laser energies, and this is attributed to an increase in the spin-lattice relaxation time T_1. Since T_1 decreases with increasing defect density,[17] this increase in T_1 with increasing laser energy might be due in part to the removal of very low defect concentrations deep in the tail of the damage distribution.[18]

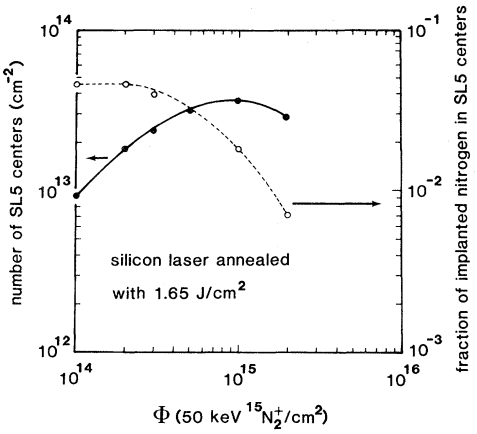

FIG. 5. Number of SL5 centers per cm^2 and the fraction of implanted N in SL5 centers plotted vs $^{15}N_2^+$ fluence for fixed $^{15}N_2^+$ implant energy and laser-anneal energy.

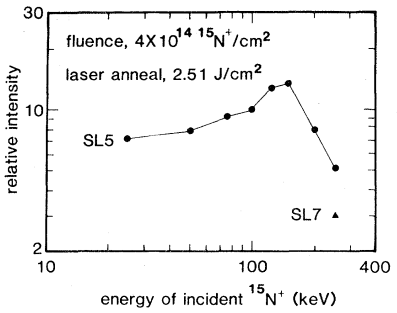

FIG. 6. Number of SL5 centers plotted vs energy of the incident $^{15}N^+$ for fixed laser-anneal energy and $^{15}N^+$ fluence.

In Fig. 5 the number of SL5 centers per cm^2 vs $^{15}N_2^+$ fluence is plotted for silicon implanted with 50-keV $^{15}N_2^+$ and laser annealed at 1.65 J/cm^2. Although the production of SL5 centers is nearly linear between 10^{14} and 3×10^{14} $^{15}N_2^+/cm^2$, the fraction of implanted N incorporated into SL5 centers is, according to our measurements, $\lesssim$5%. What fraction of the implanted nitrogen is incorporated into the silicon and into which sites (substitutional, interstitial, etc.) and defect configurations by laser annealing still needs to be determined. On the theoretical side Wood has recently developed a macroscopic theory of pulsed-laser annealing in which the impurity segregation coefficient is dependent on the melt-front velocity.[19] Consequently, the fraction of N incorporated into crystalline silicon by laser annealing might depend on melt-front velocity.

In Fig. 6, the relative number of SL5 centers versus nitrogen-implant energy is plotted. Together, Figs. 4–6 show implant and laser-anneal conditions that introduce nitrogen into SL5 centers.

An attempt was made to detect N in single-crystal germanium (*c*-Ge). In particular, samples of *c*-Ge were implanted with 3×10^{12}, 10^{13}, 3×10^{13}, 10^{14}, 3×10^{14}, 10^{15}, and 3×10^{15} $^{15}N_2^+/cm^2$ at 80 keV and laser annealed with 2.2 J/cm^2. These samples were measured at 10 K with a microwave power of -30 dBm in the dispersion and adsorption mode with and without light; however, no EPR spectrum containing ^{15}N hf lines was detected.

C. Thermal-annealing effects

If silicon containing SL5 centers introduced by implantation and laser annealing is thermally an-

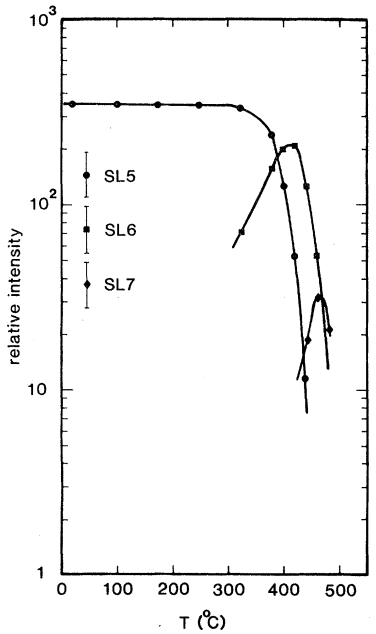

FIG. 7. Isochronal (20 min) thermal annealing of N-implanted, laser-annealed silicon.

nealed at 400 °C, another distinct nitrogen center (SL6) is observed with EPR. Since these nitrogen centers might be different due to the incorporation of another impurity, in particular C or O, we implanted silicon samples with $^{13}C^+$, $^{17}O^+$, $^{27}Al^+$, $^{31}P^+$, and $^{32}S^+$. Each of these samples was also implanted with $^{15}N^+$ (for the specific implant and laser-anneal conditions see Ref. 20). The energies were selected so as to give optimum overlap of the two implanted impurities in each sample. In addition, one sample was implanted with only $^{15}N^+$. After laser annealing all samples with 2.5 J/cm^2 the spectra in each sample were measured as a function of 20-min isochronal anneals. The results of our analysis are summarized in part in Fig. 7. Inspection of the spectra indicated that no hyperfine structure due to any of these implanted impurities (other than a single ^{15}N) was part of the SL5, SL6, or SL7 spectra. Furthermore, the intensity of these spectra was not significantly affected by any one of these impurities. However, there was one effect that emerged. In one set of samples that was implanted with (N), (N,O), and (N,C), the mean projected range of the impurities in each sample was 5000 Å, whereas in the samples implanted with (N,Al), (N,P), and (N,S), the mean projected range was 3000 Å. Our measurements indicated that the SL6 and SL7 spectra appearing in the set implanted to a mean depth of 5000 Å were enhanced in intensity over the same spectra appearing in the set implanted with impurities to a mean depth of 3000 Å. These results suggest that the residual lattice damage, which exists beyond the melt depth and was greater in the case of the 5000-Å implants as deduced from calculations by Brice,[21,22] provided an intrinsic defect that combined with the SL5 center. Thus, we suggest that residual lattice damage in the vicinity of SL5 centers enhances the formation of other N-defect centers upon annealing. The identity of these N-defect centers is considered in Sec. IV B 3.

How unique is laser annealing to the formation of paramagnetic N centers? Can paramagnetic N centers be introduced by thermal annealing of N-implanted silicon? In probing these questions four silicon samples were implanted with 10^{13}, 10^{14}, 10^{15}, and 10^{16} 200-keV $^{14}N^+$/cm^2. The EPR spectra were measured in these samples after 20-min isochronal anneals at 60,100,140, . . . , 300,350, . . . , 800,900, . . . , 1100 °C. The only spectrum observed that exhibited ^{14}N hf splittings was the SL5 spectrum, and it was observed only in the sample implanted with 10^{14} 200-keV $^{14}N^+$/cm^2 and only after the 450 °C, 20-min thermal anneal. Since this SL5 spectrum was observed in fast passage, T_1 was relatively long and suggests the absence of nearby damage defects. Thus, the evolution of other N-defects centers is probably less likely and, in fact, was not observed.

In this study we also observed two other isotropic resonances in slow passage with $g=2.0028$ and 1.9995 (± 0.0004), with $\Delta B_{pp}=2$ G. These spectra were observed in the samples implanted with 10^{15} and 10^{16} 200-keV $^{14}N^+$/cm^2 and subsequently thermally annealed at 800 °C for 20 min. These spectra were not observed in the sample implanted with

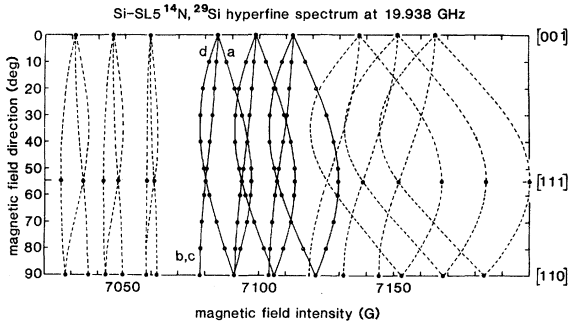

FIG. 8. Angular dependence of the ^{14}N,^{29}Si SL5 hyperfine spectrum. The branches labeled *a*, *b*, *c*, and *d* correspond to the resonances associated with particular N-Si$_i$ ($i=a,b,c,d$) and with the axis of distortion in Fig. 10.

TABLE I. Values of the $\overleftrightarrow{g}$, $\overleftrightarrow{A}(^{14}N)$ or $\overleftrightarrow{A}(^{15}N)$, and $\overleftrightarrow{A}(^{29}Si)$ coupling dyadics for the $S=\frac{1}{2}$ SL5 and SL6 spectra. The SL5 and SL6 centers are observed to be axially symmetric about the ⟨111⟩ axis.

Spectrum	$\overleftrightarrow{g}$ (±0.0004)	$\overleftrightarrow{A}(^{14}N)$ (±0.000 03 cm^{-1})	$\overleftrightarrow{A}(^{15}N)$ (±0.000 03 cm^{-1})	$\overleftrightarrow{A}(^{29}Si)$ (±0.000 03 cm^{-1})
Si-SL5	$g_{\|\|}=2.0026$	$A_{\|\|}=0.001\,51$	$A_{\|\|}=0.002\,08$	$A_{\|\|}=0.013\,26$
	$g_{\perp}=2.0089$	$A_{\perp}=0.001\,21$	$A_{\perp}=0.001\,70$	$A_{\perp}=0.007\,73$
Si-SL6	$g_{\|\|}=2.0018$	$A_{\|\|}=0.000\,78$		
	$g_{\perp}=2.0085$	$A_{\perp}=0.000\,64$		

only 10^{14} 200 keV $^{14}N^+/cm^2$. These resonances might be associated with nitrogen.

Finally, Matsumori *et al.*[23] reported observing a ^{14}N hf spectrum at 4 K with $g=2.041$ and a hf splitting of 41.4 G (presumably isotropic) in silicon implanted with 10^{15} 100-keV $^{14}N^+/cm^2$ and annealed at 800 °C for 10 min. Although we reproduced these implant and anneal conditions we were unable to detect this spectrum. The large shift in the g value reported for this isotropic spectrum, $\Delta g=0.0387$, is unprecedented for a light impurity in an s state in silicon.

IV. EPR RESULTS AND DISCUSSION

A. Spectral analysis

The SL5 spectrum for $\vec{B}||[001]$ is illustrated in Fig. 3. The relative intensity and splittings of the resolved ^{14}N or ^{15}N and ^{29}Si hf spectra arise from a single N and a single Si. The intensity of the ^{29}Si hf spectrum reflects the fact that the ^{29}Si isotope ($I=\frac{1}{2}$) is only 4.70% naturally abundant.

The angular dependence of these resolved ^{14}N and ^{29}Si hf spectra is shown in Fig. 8 and indicates that this N center has C_{3v} symmetry about the ⟨111⟩. The magnetic field $\vec{B}$ dependence of the SL5 spectrum was analyzed in terms of an $S=\frac{1}{2}$ spin Hamiltonian

$$\mathcal{H}=\mu_B\vec{B}\cdot\overleftrightarrow{g}\cdot\vec{S}+\sum_i\vec{S}\cdot\overleftrightarrow{A}_i\cdot\vec{I}_i\ , \tag{1}$$

where $\overleftrightarrow{g}$ and $\overleftrightarrow{A}_i$ characterize the Zeeman and hf interactions, respectively, and μ_B ($=4.6686\times10^{-5}$ cm^{-1}/G) is the Bohr magneton. The values of the dyadics $\overleftrightarrow{g}$ and $\overleftrightarrow{A}_i$ which characterize the SL5 spectrum are tabulated in Table I. A similar analysis was applied to the SL6 spectrum, and those results are also tabulated in Table I. The production of SL6 centers is discussed in Sec. III C.

1. Hyperfine interactions

The qualitative character of the paramagnetic orbital can be represented in terms of a one-electron molecular orbital

$$\psi=\sum_i\eta_i(\alpha_i\,|\,s\rangle+\beta_i\,|\,p\rangle)\ , \tag{2}$$

where α_i and β_i ($\alpha_i^2+\beta_i^2=1$) specify the relative admixtures of s and p character at the ith atomic site and η_i is the degree of localization. For axial symmetry (in this case $z||[111]$), these parameters are related to the hf dyadics by the relationships

$$A_{\mathrm{iso},i}=(A_{||,i}+2A_{\perp,i})/3$$
$$=\frac{16\pi}{3}\mu_B\frac{g_{Ni}\mu_N}{I_i}\,|\,\psi_{s,i}(0)\,|^2\alpha_i^2\eta_i^2 \tag{3}$$

and

$$A_{\mathrm{aniso},i}=(A_{||,i}-A_{\perp,i})/3$$
$$=\tfrac{4}{5}\mu_B\frac{g_{Ni}\mu_N}{I_i}\langle r_{p,i}^{-3}\rangle\beta_i^2\eta_i^2\ , \tag{4}$$

where g_{Ni} is the nuclear moment (in units of the nuclear magneton $\mu_N=2.5427\times10^{-8}$ cm^{-1}/G). Values for $|\psi_{s,i}(0)|^2$ and $\langle r_{p,i}^{-3}\rangle$ for N and Si, which were calculated by the Hartree-Fock method,[24] are tabulated in Table II.

A skeleton model for the SL5 center is shown in Fig. 9. For C_{3v} symmetry, symmetry arguments alone allow the paramagnetic electron to be in either

TABLE II. Tabulation of atomic parameters for valence electrons of neutral Si and N. These theoretical values were calculated by Cowan (Ref. 25) with the use of a Hartree-Fock code (Ref. 24).

Atom	$\|\psi_s(0)\|^2$ (10^{24} cm^{-3})	$\langle r^{-3}\rangle$ (10^{24} cm^{-3})
Si	25.84	13.68
N	32.51	20.38

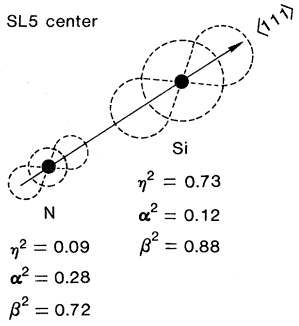

$$\Psi \simeq \sum_i \eta_i(\alpha_i|s\rangle + \beta_i|p\rangle)$$

FIG. 9. Skeleton model of the SL5 center showing the s and p character and the degree of localization of the paramagnetic electron on the N-Si which give resolved hf spectra as deduced from the data in Tables I and II.

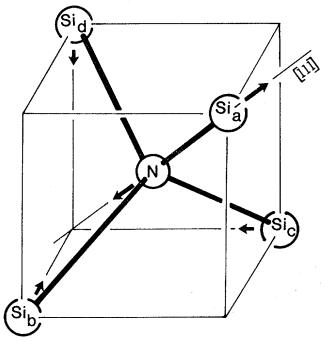

FIG. 10. Model of the SL5 center illustrating features in the molecular structure of substitutional N in silicon. The C_{3v} symmetry of this impurity is attributed to a ⟨111⟩ axial distortion in the positions of the N and neighboring silicon atoms. The arrows indicate the possible directions for atomic displacements.

an a_1- or e-symmetry state. The admixture of p_z orbitals, as deduced from the hyperfine interactions, is consistent with the electron being in an a_1 state. If the paramagnetic electron were in an e state, then occupancy by a single donor electron in this doubly degenerate level would drive a Jahn-Teller distortion lowering the symmetry from C_{3v} to C_s, and the paramagnetic orbital would consist of p orbitals perpendicular to the z axis ($z||\langle 111\rangle$). Since neither of these features is observed, the paramagnetic electron is not in the e-symmetry state. Whether this paramagnetic a_1-symmetry state is derived from the A_1 or T_2 state of the hypothetical undistorted N center with T_d symmetry is discussed in Sec. IV C.

2. Zeeman interaction

Lee and Corbett[26] have classified some of the characteristics in defect structure and bonding in terms of the anisotropy in the $\vec{\vec{g}}$ dyadic. A comparison of the anisotropy in $\vec{\vec{g}}$ for the SL5 (and SL6) center with their classification scheme suggests a defect which is either neutral or negatively charged with a paramagnetic dangling bond. In the case of the SL5 (and SL6) center the anisotropy in $\vec{\vec{g}}$ is consistent with a model in which four of the five N valence electrons covalently bond the N into a near substitutional site, and the fifth N valence electron is an antibonding paramagnetic donor electron. In our skeleton model in Fig. 9 the observed hf interactions indicate that this donor electron is highly localized on one of the nearest-neighbor Si atoms so that it appears like a ⟨111⟩ dangling bond. A lattice model for this defect is shown in Fig. 10. The fact that the N is surrounded by four silicon atoms as shown in Fig. 10 is confirmed by reorientation effects (Secs. IV B 1 and IV B 3).

B. Reorientation effects

1. Stress effects

By cooling the sample from $T \gtrsim 50$ K to $T \lesssim 25$ K under uniaxial stress along the $[\bar{1}10]$, a preferential alignment of the SL5 N centers is achieved and remains quenched in after the applied stress has been removed. By looking at the defects with the magnetic field $\vec{B}||[110]$ in Fig. 10, we observe that the resonance labeled a,d in Fig. 11 increases while the resonance labeled b,c decreases. The letters a, b, . . . correspond to the Si atom that is in common with the N-Si distortion axis and the Si atom on which the paramagnetic electron is mostly localized. Thus the N centers tend to be aligned with the paramagnetic orbital perpendicular rather than being parallel to the applied stress. This tendency is consistent with the antibonding character of this paramagnetic orbital.[27]

In an analysis similar to that for the tin-vacancy pair center by Watkins,[28] the response of the SL5 center to stress can be quantified in terms of the traceless component of the axial elastic coupling dyadic $\vec{\vec{B}}$. For the SL5 center $\vec{\vec{B}} = -3.14$ eV/(unit strain) and indicates that the energy of the defect increases upon compression along its ⟨111⟩ direction of axial symmetry. By measuring the degree of depolarization upon annealing to an intermediate

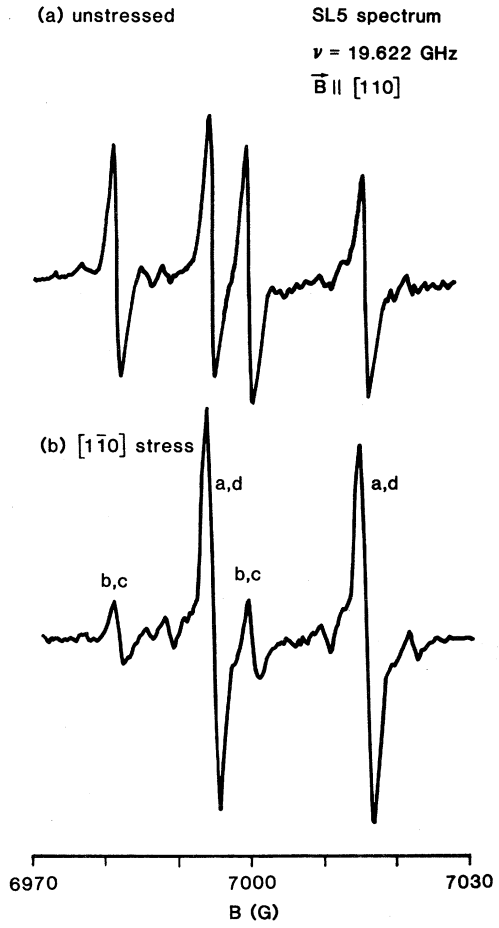

FIG. 11. Effects of [$\bar{1}$10] unaxial stress on the SL5 spectrum for $\vec{B}\|[110]$. The labels *a*, *b*, *c*, and *d* correspond to the N-Si pair in Fig. 10 on the ⟨111⟩ axis of axial symmetry.

temperature for a given time, the reorientation time of the SL5 center versus $1/T$ was determined and is plotted in Fig. 12 for $30 \lesssim T \lesssim 40$ K.

2. *Light effects*

If a stress-induced alignment is quenched in at $\simeq$10 K, we observe that incandescent light quickly randomizes this alignment. We have attempted to identify the energy of the light quanta responsible for this effect. In our earliest experiments incandescent light was passed through a silicon crystal at room temperature and into a monochromator. We reported that randomization of the quenched-in defect alignment occurred for $h\nu \gtrsim 0.58$ eV.[1] Since then further investigation has revealed that this beam was not monochromatic but contained light

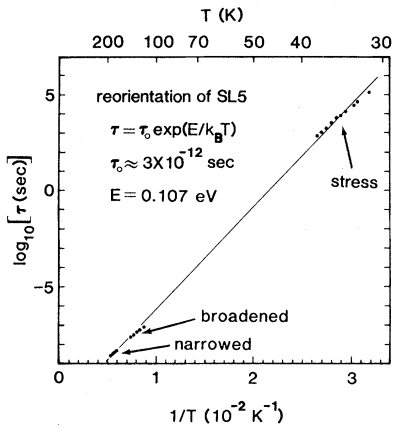

FIG. 12. Plot of the characteristic time for reorientation of the SL5 center among equivalent ⟨111⟩ distortions vs $1/T$.

with higher-order harmonics. Consequently, our earlier claim that the N center (SL5) has a donor level at 0.58 eV below the conduction band is unsupported.

In our more recent experiments the higher-energy quanta were removed by passing the light through various semiconductors. As a result of shining incandescent light through either single-crystal Ge (0.67-eV band gap) or single-crystal GaSb (0.78-eV band gap), the induced-defect alignment remains quenched in. If the light passes through single-crystal silicon at room temperature, the preferential alignment is randomized. In order to narrow this energy range the sample was illuminated by incandescent light which had passed through a single crystal of GaAs (1.3-eV band gap) and a single-grating monochromator. For $0.7 < h\nu < 1.2$ eV the higher-order harmonics were removed by the GaAs filter. The rate at which the stress-induced preferential alignment of the SL5 center is randomized was measured by EPR as a function of $h\nu$ for $0.8 < h\nu < 1.2$ eV. The results of these measurements indicate that the *dominant* mechanism which causes the N center (SL5) to reorient involves light quanta of energy between $[E(\mathrm{Si})]_{\text{band gap}} - 0.1$ eV and $[E(\mathrm{Si})]_{\text{band gap}}$. (This uncertainty in the energy of the light quanta is due to the finite resolution of the monochromator.)

Although this experiment does not reveal the details of the electronic processes that enhance the reorientation rate of the N center (SL5) under illumination at low temperature, several ideas regarding possible mechanisms are presented. In perhaps the simplest process the donor electron of the N^0 might be excited into the conduction band by a pho-

ton. The N^+ is *assumed* to relax into the undistorted substitutional site with T_d symmetry. Upon capture of a free electron, N^+ is converted to N^0 and distorts into one of four equivalent $\langle 111 \rangle$ distortions at random. In this interpretation the resonant photon energy corresponds to the position of the N^0 donor level below the conduction band.

In the second model band-gap light generates a free electron-hole pair. The hole captures the N-donor electron so that N^0 goes to N^+ and the N center relaxes from C_{3v} to T_d symmetry. Upon capture of a free electron N^+ returns to N^0 and the induced-defect alignment is randomized.

In the third model band-gap light produces free electrons and holes. The N^0 captures an electron to become N^-. This state, which has been postulated by Pantelides and Sah,[29] is *assumed* to be a shallow donor state. For a sufficiently shallow donor level the delocalization of the donor wave function allows the N^- center to relax into the undistorted substitutional site. Upon hole capture a N^- center returns to a N^0 center, and the induced N^0-center alignment is lost.

If either model two or three is operative, then model one can also occur since these three models incorporate a common process, namely, the transition of an electron between the donor level and the conduction band; however, from an experimental point of view, it is important to realize that the relative rate between competing processes may be considerably different. Thus, the process described in model one was not observed, possibly because our sub-band-gap light intensity was too weak.

Hjalmarson[30] has suggested that under band-gap illumination an exciton might become bound to the N^0 donor. Upon decay of the bound exciton, either a photon is emitted, which might account for the 1.1223-eV photoluminescence associated with N-doped silicon,[31] or the energy released upon exciton decay might provide energy for reorientation of the N^0 center.

3. *Motional effects*

Recently, Ammerlaan and Burgermeister[32] observed that the reorientation frequency versus $1/T$ for N in diamond shows large deviations from Arrhenius-type behavior for $78 < T < 200$ K. They attributed this effect to tunneling between thermally populated excited vibrational states. This observation stressed the importance of extending our measurements of the reorientation rate of N in silicon over a broader temperature range. This was achieved by measuring the motional effects on the linewidths of the resonances in the N spectrum.

The linewidth of the resonances in the SL5 N spectrum are observed to increase, except for $\vec{B} \| \langle 001 \rangle$, as the temperature increases between 100 and $\simeq$150 K. This effect is due to lifetime broadening of the resonance line. For a Lorentzian line shape that is lifetime broadened the peak-to-peak derivative linewidth ΔB_{pp} corresponds to $2/(\sqrt{3}T_2)$, where T_2 is the spin-spin relaxation time.[33] In our case T_2, which is the characteristic lifetime for phase coherence of the precessing spins in the effective magnetic field, becomes limited by the reorientation rate at sufficiently high temperatures. In this case the rate at which phase coherence of the precessing spins associated with a particular resonance and defect orientation is lost is enhanced due to reorientation of each paramagnetic electron among defect orientations whose Larmor frequencies are different.[33] For $\vec{B} \| \langle 001 \rangle$ no broadening is observed because the spins associated with the different distortion sites have the same Larmor frequency for each nuclear-spin state (Fig. 8). According to the theory developed by Gutowsky and Saika,[34] and applied to paramagnetic defects by Watkins and Corbett,[35] $T_2 = 2\tau$ for resonances in the N spectrum that are broadened but yet resolved.

For $T \gtrsim 170$ K the SL5 N spectrum is observed to be motionally averaged and narrowed into an isotropic N hf spectrum that resembles a donor electron trapped on a substitutional site with T_d symmetry. The motionally averaged and narrowed spectrum is like the spectrum observed at low temperatures ($T < 100$ K) for $\vec{B} \| [001]$. For this case, in which the jump frequency of the spins among equivalent distortions is much greater than the difference between Larmor frequencies $\delta\omega$ of the respective distortions, the loss in phase coherence between jumps becomes insignificant. For $\vec{B} \| [110]$, $\delta\omega = 2.3 \times 10^{-8}$ sec^{-1}, which corresponds to 13 G as shown in Fig. 8. For $\vec{B} \| [110]$ theory indicates that $T_2 = 4/(\tau \delta\omega^2)$, so that the resonance line narrows as τ decreases with increasing temperature. The motional narrowing of this spectrum is observed between $\simeq$170 and 185 K. The reorientation times as a function of temperature, as deduced from the effects of spectral broadening and narrowing, are also plotted in Fig. 12.

We have also compared the effects of reorientation on the SL5 and SL6 spectra as a function of temperature for $\vec{B} \| [110]$. In a silicon sample implanted with 5×10^{15} 205-keV $^{15}N^+/cm^2$, laser annealed with 2.6 J/cm^2, and thermally annealed at 410°C for 20 min, we observed both the SL5 and

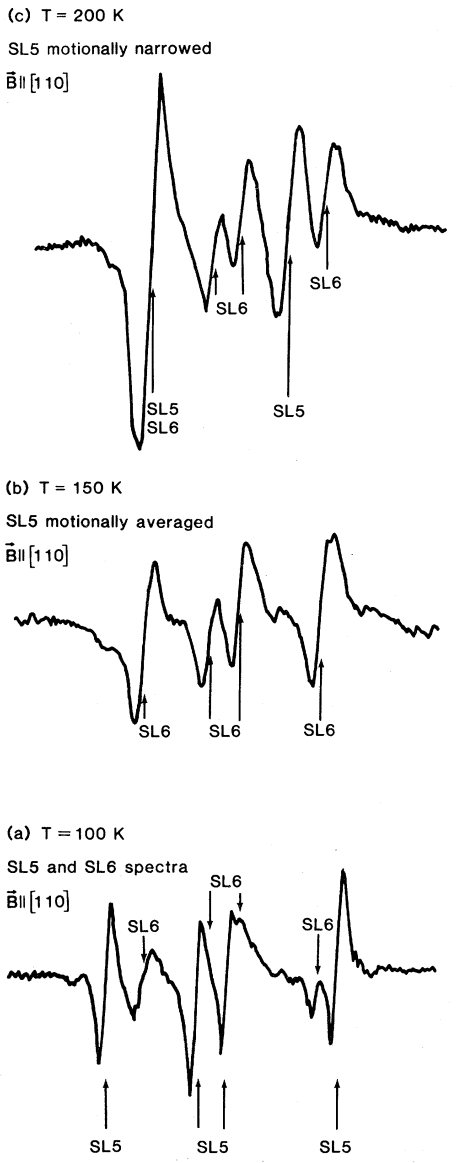

FIG. 13. Comparison of motional effects on the SL5 and SL6 spectra for $\vec{B}||[110]$ between 100 and 200 K.

SL6 spectra simultaneously (Fig. 13). Below 100 K neither the SL5 nor the SL6 spectra is visibly broadened. As the temperature is raised to $\simeq$150 K the SL5 spectrum broadens and disappears while the SL6 spectrum remains unchanged, as shown in Fig. 13. As the temperature is raised to 200 K the SL5 spectrum in Fig. 13 is observed to be motionally averaged and narrowed and reduces to the spectrum observed for $\vec{B}||[001]$, while the SL6 spectrum remains unchanged.

These results indicate that the SL6 center is more rigidly fixed in the silicon lattice than the SL5 center. This suggests that the SL6 center is an SL5 center with an additional defect nearby which is located so as to preserve C_{3v} symmetry and which pins the paramagnetic orbital and inhibits reorientation as observed. Our thermal-annealing studies (Sec. III C) also suggest that the formation of the SL6 center is enhanced by the presence of residual lattice damage upon annealing at $\approx$400 °C. To date, we have been unable to observe any dependence of the SL6 center on impurities other than a single N atom (Sec. III C).

4. *Activation energy*

A least-squares fit of the data in Fig. 12 to the Arrhenius equation

$$\tau=\tau_0\exp(E/k_BT) \tag{5}$$

indicates that $\tau_0\simeq 3\times 10^{-12}$ sec, which compares well with the expected vibration frequency $k_BT/h=10^{12}$ Hz at 50 K. The activation energy for reorientation E is 0.107 ± 0.02 eV. These data are consistent with the idea that the reorientation of the N center for $T\gtrsim 35$ K is dominated by thermal activation.

This relatively small activation energy and the high vibrational frequency factor τ_0^{-1} are suggestive of electronic effects rather than of atomic motion involving diffusional jumps.[36] These results indicate that the N atom in the SL5 centers is near the center of rotation. We presently believe that the reorientation simply involves the reorientation of the paramagnetic donor wave function and the axial distortion in the positions of the N atom and neighboring silicon atoms from one ⟨111⟩ axis to another.

C. Electronic structure

One of the first theoretical works to anticipate the deep-level character of N in silicon was that of Pantelides and Sah,[29] who predicted that the donor electron of substitutional N^0 assuming T_d symmetry would be an A_1-symmetry state with an ionization energy of 335.9 meV. An ionization energy of 52.5 meV was also predicted for N^- (diamagnetic),[29] which they suggested might explain the shallow n-type character of nitrogen-doped silicon observed by Zorin, Pavlov, and Tetel'baum[5] and by others.[7] More recently, Hjalmarson, Vogl, Wolford, and Dow[37] used a semiempirical Koster-Slater method to calculate various features in the electronic structure of substitutional N in silicon assuming

T_d symmetry. Their results also indicated that the paramagnetic donor electron is an antibonding, host like A_1 state whose level is in the middle of the band gap.[37]

The actual substitutional N center in silicon is observed by EPR to have a $\langle 111 \rangle$ axial distortion which we initially interpreted as arising from a Jahn-Teller effect.[1] Theoretical calculations of this model were performed by Vergés.[38] This interpretation has raised questions regarding the order of the A_1 and T_2 levels and the origin of the driving force for the distortion. Recently, these and other questions have been the focal point of several theoretical studies pertaining to N in diamond. These studies are of interest to us as well because of the similarities of N in silicon and diamond.

Bachelet, Baraff, and Schlüter[39] have calculated, with the use of a self-consistent Green's-function technique, various features in the electronic structure of substitutional nitrogen in diamond assuming T_d symmetry. Their calculations indicate that the paramagnetic electron occupies the A_1 antibonding state with the T_2 resonance 2–3 eV higher. Also, they find that the A_1 bound state, as well as the T_2 resonance state, is mainly carbon dangling-bond-like with some nitrogen admixture; this feature in the paramagnetic wave function is observed experimentally for N in both diamond and silicon. To account for the observed distortion with the paramagnetic electron in an A_1 state, for which a linear Jahn-Teller effect is impossible in this model, Bachelet, Baraff, and Schlüter suggest that strong, nonlinear chemical-bonding effects are responsible.

In one of the first cluster calculations, which used the extended Hückel theory (EHT), Messmer and Watkins[40] observed that an a_1 level emerged from the T_2 resonance in the conduction band upon imposing a trigonal distortion on the N center in diamond which was occupied by the paramagnetic electron. Very recently, Lannoo[41] has reexamined this conclusion and indicates that the inverted order predicted by EHT was due to an overestimation of the parameters involving the s state. For the case of normal ordering ($E_{A_1} < E_{T_2}$) Lannoo indicates that distortions can still be driven by virtue of intralevel and interlevel coupling within the A_1 and T_2 system.[41]

Fowler, Deleo, and Watkins[42] have predicted distortions for substitutional O, N, S, and C in silicon based on molecular-orbital calculations of impurity–Si_4-H_{12} clusters which are consistent with experimental observation. $X\alpha$ scattered-wave calculations were also performed on these clusters and provide information about the electronic structure. The results of these calculations indicate that substitutional N^+ in silicon occupies the substitutional site with T_d symmetry; however, substitutional N^0 occupies an off-center site on the $\langle 111 \rangle$ axis with the donor electron in an a_1 antibonding state derived from the A_1 manifold.

V. CONCLUSIONS

In this paper two aspects of our EPR studies on N in silicon have been emphasized. One is concerned with the production of paramagnetic N centers, and the other deals with the identity and structure of these N centers. The SL5 spectrum is observed by EPR to be the dominant N center introduced into silicon upon laser annealing of either amorphous or crystalline silicon implanted with N. A wide variety of implant and laser-anneal conditions for which SL5 centers are observed to be formed in silicon are summarized in Figs. 4–6. For pulsed-ruby-laser annealing our results indicate that only a small fraction of the implanted N ($\lesssim 10\%$) is quenched into SL5 centers upon regrowth from the melt. Thermal annealing between 380 and 450 °C of ion-implanted, laser-annealed samples containing SL5 centers results in the formation of two other N centers (SL6 and SL7). No evidence can be found that impurities such as O, C, P, Al, or S are incorporated into either the SL5, SL6, or SL7 centers; however, the production of the SL6 and SL7 centers appears to be enhanced by the effects of thermal annealing on the implantation lattice damage which exists beyond the silicon regrowth region. The SL5 center is also observed to be formed upon thermal annealing at $\simeq$450 °C for 20 min of crystalline silicon implanted with N.

The existence of a N atom in the SL5 center is established unambiguously through the isotropic implantation doping of ^{14}N and ^{15}N and the nature of the N hyperfine structure. Our analysis indicates that the N atom in the SL5 (and SL6) center is in a substitutional site; however, unlike the other group-V donors (P,As,Sb,Bi) the SL5 N center has C_{3v} symmetry. We observe that the $\langle 111 \rangle$ axis of C_{3v} symmetry of the SL5 center is thermally activated for T at least $\gtrsim 35$ K from one $\langle 111 \rangle$ axis to another. The characteristic time for reorientation is fitted reasonably well by the Arrhenius expression $\tau = \tau_0 \exp(E/k_B T)$. The activation energy for reorientation of the SL5 center is $E = 0.11 \pm 0.02$ eV; the preexponential factor is $\tau_0 \sim 3 \times 10^{-12}$ sec.

This low activation energy and small preexponential factor is consistent with a model which simply involves reorientation of the wave function and the ensuing distortion in atom locations. We had originally attributed this distortion to a Jahn-Teller effect. Recent theoretical considerations for N in silicon and diamond suggest that the A_1 level is lower than the T_2 level and that the paramagnetic electron is in an a_1 state originating from the A_1 rather than the degenerate T_2 manifold. Lannoo[41] and Fowler, DeLeo, and Watkins[42] have suggested that, even for $E(A_1) < E(T_2)$, a distortion may exist by virtue of intralevel and interlevel coupling within the A_1-T_2 system of states. The strong localization of the paramagnetic electron on Si-N as deduced from the hf interactions indicates that N^0 is a deep-level impurity in silicon. At this time, the location of the donor level remains unknown, contrary to our earlier assertion.[1]

ACKNOWLEDGMENTS

The assistance of Roger Shrouf, who provided the numerous implants, laser anneals, and EPR measurements for study, is gratefully acknowledged. Appreciation is expressed to Dr. Robert D. Cowan of the Los Alamos Scientific Laboratory, who provided us with the results of a Hartree-Fock calculation for Si and N. This work has been performed at Sandia National Laboratories and supported by the U.S. Department of Energy under Contract No. DE-AC04-76DP00789.

[1] K. L. Brower, Phys. Rev. Lett. 44, 1627 (1980).
[2] W. V. Smith, P. P. Sorokin, I. L. Gelles, and G. J. Lasher, Phys. Rev. 115, 1546 (1959).
[3] W. Kaiser and C. D. Thurmond, J. Appl. Phys. 30, 427 (1959).
[4] P. V. Pavlov, E. I. Zorin, D. I. Tetel'baum, and Yu. S. Popov, Dok. Akad. Nauk SSSR 163, 1128 (1965) [Sov. Phys.—Dokl. 10, 786 (1966)].
[5] E. I. Zorin, P. V. Pavlov, and D. I. Tetel'baum, Fiz. Tekh. Poluprovodn. 2, 131 (1968) [Sov. Phys.—Semicond. 2, 111 (1968)].
[6] J. B. Mitchell, P. P. Pronko, J. Shewchun, and D. A. Thompson, J. Appl. Phys. 46, 332 (1975).
[7] J. B. Mitchell, J. Shewchun, D. A. Thompson, and J. A. Davies, J. Appl. Phys. 46, 335 (1975).
[8] A. G. Cullis, H. C. Webber, and P. Bailey, J. Phys. E 12, 688 (1979).
[9] K. L. Brower, Rev. Sci. Instrum. 48, 135 (1977).
[10] K. L. Brower and P. S. Peercy, in *Laser and Electron Beam Processing of Materials,* edited by C. W. White and P. S. Peercy (Academic, New York, 1980), p. 441.
[11] The concentrations in Fig. 2 of Ref. 12 should be reduced by a factor of 2.7.
[12] K. L. Brower, in *Defects and Radiation Effects in Semiconductors, 1980,* in the Eleventh International Conference on Defects and Radiation Effects in Semiconductors, Oiso, Japan, 1980, edited by R. R. Hasiguti (IOP, London, 1981), p. 491.
[13] J. A. Knapp (private communication).
[14] T. Hirao, K. Inoue, S. Takayanagi, and Y. Yaegashi, J. Appl. Phys. 50, 193 (1979).
[15] R. O. Bell, M. Toulemonde, and P. Siffert, Appl. Phys. 19, 313 (1979).
[16] G. J. Galvin, M. O. Thompson, J. W. Mayer, R. B. Hammond, N. Paulter, and P. S. Peercy, Phys. Rev. Lett. 48, 33 (1982).
[17] K. L. Brower, and W. Beezhold, J. Appl. Phys. 43, 3499 (1972).
[18] M. S. Skolnick, A. G. Cullis, and H. C. Webber, in *Laser and Electron-Beam Solid Interactions and Materials Processing,* edited by J. F. Gibbons, L. D. Hess, and T. W. Sigmon (North-Holland, New York, 1981), p. 185.
[19] R. F. Wood, Phys. Rev. B 25, 2786 (1982).
[20] Sample No. 1: 3×10^{13} 239-keV $^{31}P^+/cm^2$; sample No. 2: 3×10^{13} 215-keV $^{27}Al^+/cm^2$; sample No. 3: 3×10^{13} 247-keV $^{32}S^+/cm^2$. Samples Nos. 1—3 were also implanted with 3×10^{15} 118-keV $^{15}N^+/cm^2$. The mean projected range of these implanted impurities in samples Nos. 1—3 is 3000 Å. Sample No. 4: 5×10^{13} 178-keV $^{13}C^+/cm^2$; sample No. 5: 5×10^{13} 233-keV $^{17}O^+/cm^2$; sample No. 6: blank. Samples Nos. 4—6 were also implanted with 5×10^{15} 205-keV $^{15}N^+/cm^2$. The mean projected range of these implanted impurities in samples Nos. 4—6 is 5000 Å. Samples Nos. 1—6 were pulsed-ruby-laser annealed with 2.51 ± 0.02 J/cm^2.
[21] D. K. Brice (private communication).
[22] D. K. Brice, *Ion Implantation Range and Energy Deposition Distributions* (IFI Plenum, New York, 1975), Vol. 1.
[23] T. Matsumori, K. Takeda, T. Kobayashi, H. Maekawa, and T. Izumi, Tokai Daigaku Kiyo Kogaku 1, 1 (1972).
[24] D. C. Griffin, R. D. Cowan, and K. L. Andrew, Phys. Rev. A 3, 1233 (1971).
[25] R. D. Cowan (private communication).
[26] Y. H. Lee and J. W. Corbett, Phys. Rev. B 8, 2810 (1973).
[27] G. D. Watkins and J. W. Corbett, Phys. Rev. 121, 1001 (1961).
[28] G. D. Watkins, Phys. Rev. B 12, 4383 (1975).
[29] S. T. Pantelides and C. T. Sah, Phys. Rev. B 10, 638 (1974).
[30] H. P. Hjalmarson (private communication).
[31] M. Tajima, T. Masui, T. Abe, and T. Nozaki, Jpn. J. Appl. Phys. 20, L423 (1981).
[32] C. A. J. Ammerlaan and E. A. Burgermeister, Phys.

Rev. Lett. 47, 954 (1981).
[33]A. Carrington and A. D. McLachlan, *Introduction to Magnetic Resonance* (Harper and Row, New York, 1967), pp. 10 and 205.
[34]H. S. Gutowsky and A. Saika, J. Chem. Phys. 21, 1688 (1953).
[35]G. D. Watkins and J. W. Corbett, Phys. Rev. 134, A1359 (1964).
[36]For example, the typical activation energy for electronic reorientation of several centers in silicon is the following: negative vacancy oxygen, 0.38 eV; positive divacancy, 0.073 eV; negative divacancy, 0.056 eV; vacancy $\sim 0.01-0.02$ eV; phosphorous vacancy, 0.062 eV; carbon pair, 0.20 eV. The activation energy for atomic reorientation is generally $\gtrsim 1$ eV.
[37]H. P. Hjalmarson, P. Vogl, D. J. Wolford, and J. D. Dow, Phys. Rev. Lett. 44, 810 (1980).
[38]J. A. Vergés, J. Phys. C 14, 365 (1981).
[39]G. B. Bachelet, G. A. Baraff, and M. Schlüter, Phys. Rev. B 24, 4736 (1981).
[40]R. P. Messmer and G. D. Watkins, Phys. Rev. B 7, 2568 (1973).
[41]M. Lannoo, Phys. Rev. B 25, 2987 (1982).
[42]W. B. Fowler, G. G. Deleo, and G. D. Watkins, Bull. Am. Phys. Soc. 27, 279 (1982).